Journal of Materials Chemistry C

Accepted Manuscript

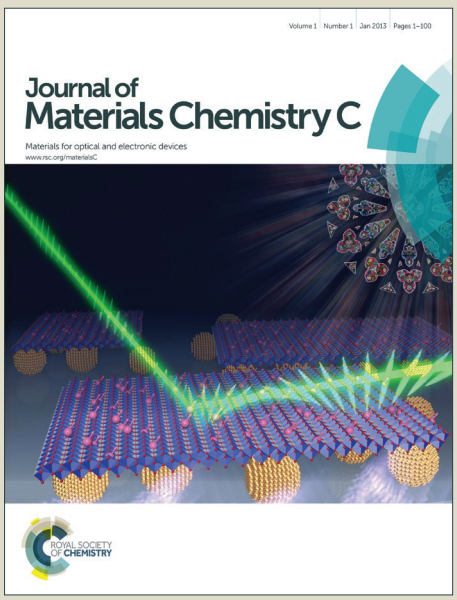

ROYAL SOCIETY OF CHEMISTRY

www.rsc.org/materialsC

A Synergistic Combination of Diatomaceous Earth with Au Nanoparticles as a Periodically Ordered, Button-like Substrate for SERS Analysis of the Chemical Composition of Eccrine Sweat in Latent Fingerprints

Jing Chen[1], *Gaowu Qin*[1,*], *Qing Chen*[2], *Jiangyu Yu*[3], *Song Li*[1], *Feng Cao*[1], *Bo Yang*[1], *Yuping Ren*[1]

1. Key Laboratory for Anisotropy and Texture of Materials (Ministry of Education), Northeastern University, Shenyang 110819, China

2. Research Center for Analytical Sciences, College of Sciences, Northeastern University, Shenyang 110819, China

3. College of Materials and Metallurgy, Northeastern University, Shenyang 110819, China

***Corresponding author**

Tel.: +86 24 83691565 *E-mail: qingw@smm.neu.edu.cn

Abstract

The artistry and the amazingly beautiful hierarchical three-dimensional (3D) patterning of diatoms make them an ideal biological scaffold. Here, fraction-free and ultra-high-purity diatomaceous earth has been successfully prepared by low speed centrifugation in saturated sucrose solution and calcination at 600 ^{o}C for 2 h. The

prepared citrate-stabilized 18±2.4 and 32±5.4 nm Au nanoparticles were singly, uniformly and densely self-assembled onto amino-functionalized diatomaceous earth templates following their surface morphologies *via* electrostatic interactions, during which the control experiment and appropriate parameter exploration were performed. The formed 18±2.4 and 32±5.4 nm Au nanoparticle coated diatomaceous earth fine-grained composite materials were pressed into hard, button-like tablets with a fixed diameter of 13 mm and a thickness of 2 mm, and then the two fabricated types of button-like portable tablets were used for surface-enhanced Raman spectroscopy (SERS) detection, and their enhancement factors (EFs), SERS reproducibility and long-term stability were testified using rhodamine 6G (R6G) as the probe molecule. The button-like portable tablet composed of diatomaceous earth-templated 32±5.4 nm Au nanoparticle arrays had a higher EF and was successfully applied to SERS analysis of the trace chemical composition of eccrine sweat in latent fingerprints. It may reveal the medical condition of an individual by analyzing the obtained SERS spectra, suggesting that the SERS-based methodology, due to its high sensitivity, has potentially wide applications in fields that need trace detections, such as medical diagnostics and forensic investigations. Moreover, the button-like, 3D periodically ordered tablet as a portable SERS substrate composed of a synergistic combination of diatomaceous earth with Au nanoparticles in this work is robust, easy to carry around, and applicable to on-site SERS detection.

1. Introduction

The visualization and identification of latent fingerprints plays an important role in

forensic investigations, access control, and individual credentials due to the uniqueness of fingerprints to each person.[1,2] Traditional visualization means of latent fingerprints include magnetic filings dusting, iodine fuming, silver nitrate fuming, ninhydrin fuming, and cyanoacrylate fuming.[2-5] Recently, with developments in nanotechnology, nanomaterials (such as quantum dots, metal nanoparticles) and advanced approaches (such as electrochemiluminescence and spectral imaging techniques) have been successfully applied in the visualization of latent fingerprints to enhance the sensitivity and contrast.[6-11] In addition to gaining patterns from latent fingerprints, investigation of the chemical composition of latent fingerprints is also of great importance, as by analyzing metabolites in sweat and exogenous contaminations in latent fingerprints, the physical condition of an individual, drugs of abuse, explosive residues and other specific chemical information can be detected.

The chemical composition of a latent fingerprint is a complex mixture of eccrine sweat secreted directly onto the fingers[12] as well as contaminants from touching areas of the body or the environment. The detection of contaminants present in latent fingerprints such as sebum, illicit drugs, and explosive particles has been extensively studied by using ultraviolet fluorescence spectroscopy, gas chromatography-mass spectrometry (GC-MS), Fourier transform infrared spectroscopy (FTIR), and Raman spectroscopy.[12-18] Pure eccrine sweat consists of water, inorganic salts (such as sodium chloride and potassium chloride) and organic compounds (such as amino acids, polypeptides, proteins, glucose, and urea).[12] However until now, there have been few reports on the analysis of the chemical composition of eccrine sweat in

latent fingerprints, such as amino acids, proteins and polypeptides, although they may contain more biological and medical information that can be further used for medical diagnostics.

Surface-enhanced Raman spectroscopy (SERS) is an ultra-sensitive, nondestructive, and fast analytical technique that can offer rich and distinguishable vibrational information used for molecule identification and can fulfill trace detection or even single molecule detection.[19,20] Moreover, SERS requires little or no sample preparation, and water is a weak Raman scatterer, leading to little or no interference in SERS detection. All of the above features make SERS an ideal spectroscopy technique for analyzing the chemical composition of eccrine sweat in latent fingerprints.

Despite the prominent progress of SERS in recent years, developing novel Au, Ag SERS nanostructures with three-dimensional (3D) ordered geometries and highly enhanced capabilities over large areas still remains an active research pursuit.[21-26] Lithographic techniques, especially electron beam lithography (EBL), have proven effective in the generation of periodic SERS arrays.[27-32] However, the lithographically produced SERS arrays normally have moderate enhancement factors (EFs, ~10^5-10^6), and the low-throughput, significant cost, and low efficiency of these techniques make the generation of large areas of SERS sensing platforms extremely difficult.[33-35] An alternative approach to obtain finely controlled SERS plasmonic nanostructures is the template-mediated fabrication technique, in which the assembly of nanoparticles onto template surfaces can be fulfilled by in situ growth, nonspecific

adsorption, or specific interaction so that larger-scale SERS structures can be produced.[36,37] Biological materials such as bacteria,[38] viruses,[39] fungi,[40] and diatoms,[41] whose intrinsically sophisticated architectures provide uniquely species-specific details that man-made templates can hardly offer, have been exploited as ideal templates.[37]

Diatoms, a form of single cell photosynthetic algae, are encased within two half cell walls made of amorphous hydrated silica called "frustule".[42,43] Diatoms possess a combination of structural, optical, chemical, mechanical features[44] and have found application in catalysis, optics, microfluidics, drug delivery, and separation science.[45-48] Here, the artistry and the amazingly beautiful hierarchical 3D patterning of diatom silica shells, together with their good biocompatibility and potential for chemical functionalization, make diatoms the ideal biological scaffold for assembling Au and Ag nanoparticles. The obtained biohybrid materials will exhibit good properties and have broad applications as they combine the morphological characteristics of diatoms with the properties of nanoparticles. Payne *et al*. reported silver-coated diatoms and 3D free-standing silver microshell diatom replicas produced by thermal evaporation, and their SERS EFs were calculated to be 10^5~10^6 by using rhodamine 6G (R6G) as the analyte.[37] In Jantschke's work, three types of diatom-templated noble metal nanoparticle (Pt, Au, and Ag, with their diameters all less than 10 nm) arrays were prepared by layer-by-layer deposition or covalent linking, and the SERS EF of the diatom-templated Ag nanoparticle arrays was calculated to be 2×10^3.[45] In Rosi's paper, the sequence-specific assembly of nanoparticles was

performed by DNA-functionalized diatoms interacting with complementary DNA-functionalized 13 nm Au nanoparticles.[36]

Although the above reports have demonstrated that several protocols could be used for the fabrication of diatom-templated SERS arrays, there still exist limitations. For example, the uniform distribution of Au or Ag nanoparticles on the diatom templates cannot be well controlled by employing the physical deposition technique. Moreover, Au or Ag nanoparticles will deposit on only one side of the diatoms due to the limitations of the physical deposition technique. Thus, the reproducibility and homogeneity of the SERS signals cannot be guaranteed. The specific adsorption technique will ensure the uniform assembly of Au or Ag nanoparticles onto the diatoms, but they require complex operation procedures (such as DNA or protein-modification) and are normally involved with small Au or Ag nanoparticle (diameters less than 14 nm) attachment, which is not the ideal size for SERS detections.

In this work, two different sizes of citrate-stabilized Au nanoparticles (18±2.4 nm, 32±5.4 nm) were singly, uniformly and densely assembled onto fraction-free and ultra-high-purity amino-functionalized diatomaceous earth templates *via* electrostatic interactions, respectively. Then, the prepared Au nanoparticle coated diatomaceous earth granulated composite materials were pressed into button-like portable tablets for the SERS analysis of the trace chemical composition of eccrine sweat in latent fingerprints. The EF, reproducibility and long-term stability of the 3D periodically ordered diatomaceous earth-templated Au nanoparticle substrates were also evaluated.

The advantages and improvements of the fabrication technique used in this work are listed below. (1) Different from by employing living diatoms as templates, in our work, a large and cost-effective source of diatom silica, diatomaceous earth, was used as the template. Diatomaceous earth is not an earth but is formed by the accumulation of the fossil siliceous frustules of diatoms, which is ready-made, without needing to be cultivated further.[43,44] (2) A strong relationship exists between the Au nanoparticles size and their SERS effect due to the variation of the localized surface plasmon (LSP) with the nanoparticle size.[49] It is generally accepted that Au nanoparticles of tens of nanometers in size will have better SERS activities.[50-53] However, the uniform attachment and distribution of Au nanoparticles onto templates will become harder as the nanoparticle size becomes larger. Here, compared to previous work on diatom-templated small Au nanoparticle (diameters usually less than 14 nm with weak SERS capabilities) arrays, two relatively larger Au nanoparticles with moderate sizes of 18±2.4 nm and 32±5.4 nm were produced. Thus, both higher SERS enhancements and good attachment and distribution will be guaranteed at the same time. (3) The two different sizes of Au nanoparticles were densely coated in an ordered fashion onto diatomaceous earth by electrostatic interactions, one simple but powerful technique. Moreover, dense adsorption creates numerous “hot spots” and thus ensures high SERS enhancement; ordered assembly means that good reproducibility will be fulfilled. (4) The above fabricated granulated composite materials were pressed into button-shaped portable SERS tablets with a fixed diameter of 13 mm and a thickness of 2 mm, that are robust, easy to carry

around, and suitable for on-site SERS detections.

2. Experimental Section

2.1 Chemicals and Materials

Diatomaceous earth (food-grade) was collected from Changbai, Jilin Province, China. $HAuCl_4 \cdot 4H_2O$, trisodium citrate dihydrate ($Na_3C_6H_5O_7 \cdot 2H_2O$), NaOH, HCl, ethanol, glacial acetic acid, sucrose were all of analytical grade and purchased from Sinopharm Chemical Reagent Co., Ltd. (3-Aminopropyl)triethoxysilane (APTES, 98%) was purchased from Aladdin Industrial Inc.. Rhodamine 6G (R6G) (≥ 95.0%, analytical standard) was purchased from Sigma-Aldrich. Ultrapure water (18.2 MΩ·cm) was used throughout the experiments. All reagents were used without further purification. All glassware used was cleaned in freshly prepared aqua regia solution (HCl/HNO_3, 3:1), then rinsed thoroughly with H_2O before use.

2.2 Functionalization of Diatomaceous Earth Surfaces

2.2.1 Separation of Diatomaceous Earth

To remove diatomaceous earth fractions, separation procedures were performed. An appropriate amount of diatomaceous earth was put into a saturated sucrose solution, and low speed centrifugation was performed at 500×g for 5 min. Then, the supernatant was discarded, and the bottom diatomaceous earth was collected and put into the saturated sucrose solution again. The above procedure was repeated two more times, and the final bottom diatomaceous earth was copiously washed with water *via* centrifugation.

2.2.2 Purification of Diatomaceous Earth

After the separation procedure, diatomaceous earth was further processed by calcination at 600 ^{o}C for 2 h to remove the organic components and impurities, both on the surface and in the pores of the fossil diatom frustules.

2.2.3 Surface Modification of Diatomaceous Earth

The above processed diatomaceous earth (2 g) was well-suspended in a mixture of ethanol (100 mL) and ultrapure water (2 mL) by ultrasonication, followed by vigorous stirring in a 35 ^{o}C water bath. Then, a solution containing 10 mL of ethanol, 2 mL of APTES, and 100 μL of glacial acetic acid (to activate the diatomaceous earth cell walls) was added dropwise into the above suspension, and the reaction was allowed to run for another 12 h. The precipitate was collected *via* centrifugation and washed in ethanol three times.

2.3 Synthesis of Gold Nanoparticles

2.3.1 Synthesis of 18 ±2.4 nm Au Nanoparticles[54]

A solution of 150 mL, 2.2 mM of sodium citrate in a 250 mL three-necked flask was brought to boil while being stirred, and 1 mL of 25 mM $HAuCl_4$ was injected. The reaction was allowed to run until the solution reached a wine red color. A condenser was used to prevent the evaporation of the solvent.

2.3.2 Synthesis of 32 ±5.4 nm Au Nanoparticles[55]

A 100 mL, 0.25 mM of aqueous $HAuCl_4$ was prepared in a 250 mL three-necked flask, and HCl (1 M) or NaOH (1 M) were added to adjust the solution pH to reach 7.0. Then the solution was heated to boil while being stirred, and 490 μL of 5% sodium citrate solution was added immediately. The reaction was allowed to run until the

solution reached a wine red color. A condenser was used to prevent the evaporation of the solvent.

2.4 Assembly of Au Nanoparticles onto Amino-functionalized Diatomaceous Earth Templates

To make the Au nanoparticles present with a greater monodispersity on the diatomaceous earth surface, an appropriate amount of ethanol was added into the above citrate-stabilized Au nanoparticle aqueous solution to make the volume ratio of water : ethanol 4 : 1.[56] Then, the amino-functionalized diatomaceous earth (0.025 g) was added into the above mixture and ultrasonication was used to make the amino-functionalized diatomaceous earth well-dispersed, followed by continuous stirring for 24 h. The precipitate was collected *via* centrifugation (3000×g, 5 min) and washed with water and ethanol three times.

2.5 Fabrication of Portable SERS Substrates

The above Au nanoparticle coated diatomaceous earth granulated composite material was pressed into hard tablets by a tablet press for the following SERS detection. The two punches and a die in the tablet press were cleaned with acetone and ethanol before use. The formed SERS tablets were placed in sterile petri dishes in the dark at room temperature prior to use.

2.6 SERS Signal Reproducibility and Enhancement Capability Measurement

R6G was used as the probe molecules. 10 μL of 10^{-4} M R6G solution was dripped onto a portable SERS tablet, and SERS spectra were acquired immediately after the substrate was dried under ambient conditions. Normal Raman spectrum of 10^{-2} M

R6G solution was also acquired.

2.7 SERS Analysis of the Chemical Composition of Eccrine Sweat in Latent Fingerprints

Hands were washed using ordinary soap and water and dried with a paper towel. Then, one hand was enclosed in a disposable PE glove, and a rubber band was used to fasten the end of the glove to let the hand sweat. Next, one of the sweaty fingers was pressed onto the portable SERS tablet, and the SERS spectra were acquired immediately from the latent fingerprint. Tweezers cleaned by acetone and ethanol were used to move the SERS tablet.

2.8 Long-term Stability Measurement of SERS Substrates

After 90 days, the button-like portable SERS tablets composed of diatomaceous earth-templated 18±2.4 and 32±5.4 nm Au nanoparticle arrays which were stored in sterile petri dishes in the dark were carefully taken out to test their SERS performance. R6G was employed as the probe molecules, and 10 μL of 10^{-4} M of R6G solution was dropped onto each SERS tablet.

2.9 Characterization

Transmission electron microscopy (TEM) observations of the samples were performed using JEM-2100F, JEOL, with the acceleration voltage of 200 kV. Field emission scanning electron microscopy (FE-SEM) was carried out on JSM-7001F, JEOL, with the operation voltage of 15kV. The confocal laser scanning microscope (Olympus LEXT OLS3100) was carried out to get the images of diatomaceous earth. All SERS and bulk spectra were obtained using a confocal Raman spectrometer

(Horiba Scientific, XploRA ONE) equipped with a 638 nm laser and a 50× objective. The incident laser power was attenuated to 0.1 mW or 1 mW for SERS spectra acquisitions, and the laser power for the normal Raman spectrum acquisition of 10^{-2} M bulk R6G solution was set as 10 mW. The frequency of the Raman instrument was calibrated by referring to a silicon wafer at the vibrational band of 520.7 cm^{-1}. All the measurements were carried out under ambient conditions. Ultraviolet-visible (UV-vis) absorption spectra were recorded using a Shimadzu UV-2100 UV-vis spectrophotometer. Zeta potential measurements were performed using Zetasizer Nano ZS system from Malvern. Fourier transform infrared (FT-IR) spectra were recorded using a Spectrum One spectrometer (Perkin Elmer Co., USA). Specific surface area was measured by a surface area and porosity analyzer (TriStar Ⅱ 3020, Micromeritics Instrument Corporation).

3. Results and Discussion

3.1 Separation and Purification of Diatomaceous Earth.

3.1.1 Separation of Diatomaceous Earth

Raw diatomaceous earth contains fractions and impurities, and separation and purification procedures are necessary before the diatomaceous earth is modified. The fossil diatom frustule fractions and the intact fossil diatom frustules in raw diatomaceous earth would have different sedimentation rates when they were centrifuged in viscous saturated sucrose solution, as they had different sizes. The intact fossil diatom frustules would have a higher sedimentation rate due to their larger size, whereas the fossil diatom frustule fractions would have a lower

sedimentation rate due to their smaller size; thus, within the same centrifugation time, the separation of diatomaceous earth could be fulfilled, as the fractions and the intact diatom frustules would be located in different layers of the saturated sucrose solution following the low speed centrifugation. Figure 1a, 1b are the corresponding confocal laser images of the raw diatomaceous earth and raw diatomaceous earth after separation. Figure 1a shows that the raw diatomaceous earth is a mixture of fractions and the intact remains of dead diatoms that still maintain their shapes. Then, a separation procedure was performed to remove the unwanted fraction sediments. Large numbers of disc-shaped diatoms remain present in Figure 1b, indicating that a great part of the fossil diatom frustules fractions has been effectively removed by the low speed centrifugation in the saturated sucrose solution.

3.1.2 Purification of Diatomaceous Earth

To further remove organic components and impurities and to activate the fossilized diatom frustules, the diatomaceous earth after the separation procedure was processed by calcination at 600 ^{o}C for 2 h. The temperature of 600 ^{o}C was chosen because at this temperature, the organic portions and most of the impurities in the fossil diatom frustules can be removed without damaging their delicate morphology and surface hydroxy.[57] Figure 1c presents the FT-IR spectra of diatomaceous earth before and after calcination at 600 ^{o}C for 2 h. The band at 3433 cm^{-1} corresponds to the O-H and/or N-H stretching vibrations, while the weak bands at 2924 and 2851 cm^{-1} are related to the asymmetric and symmetric stretching vibrations of the C-H bond. The band at 1636 cm^{-1} can be assigned to the N-H bending vibration, while the band at

1083 cm^{-1} is ascribed to the Si-O stretching vibration. After being calcined at 600 ^{o}C for 2 h, the peaks at 2924 and 2851 cm^{-1} were gone, and the bands at 3433 and 1636 cm^{-1} were reduced, indicating that most of the organic components have been effectively removed. Figure 1d and 1e are the FE-SEM images of an intact fossil diatom frustule before and after calcination, respectively. After being calcined at 600 ^{o}C for 2 h, the diatom fossil presented a sculptured discoid form with a clean surface. Thus, the fraction-free and ultra-high-purity diatomaceous earth was prepared and was ready for the following modification.

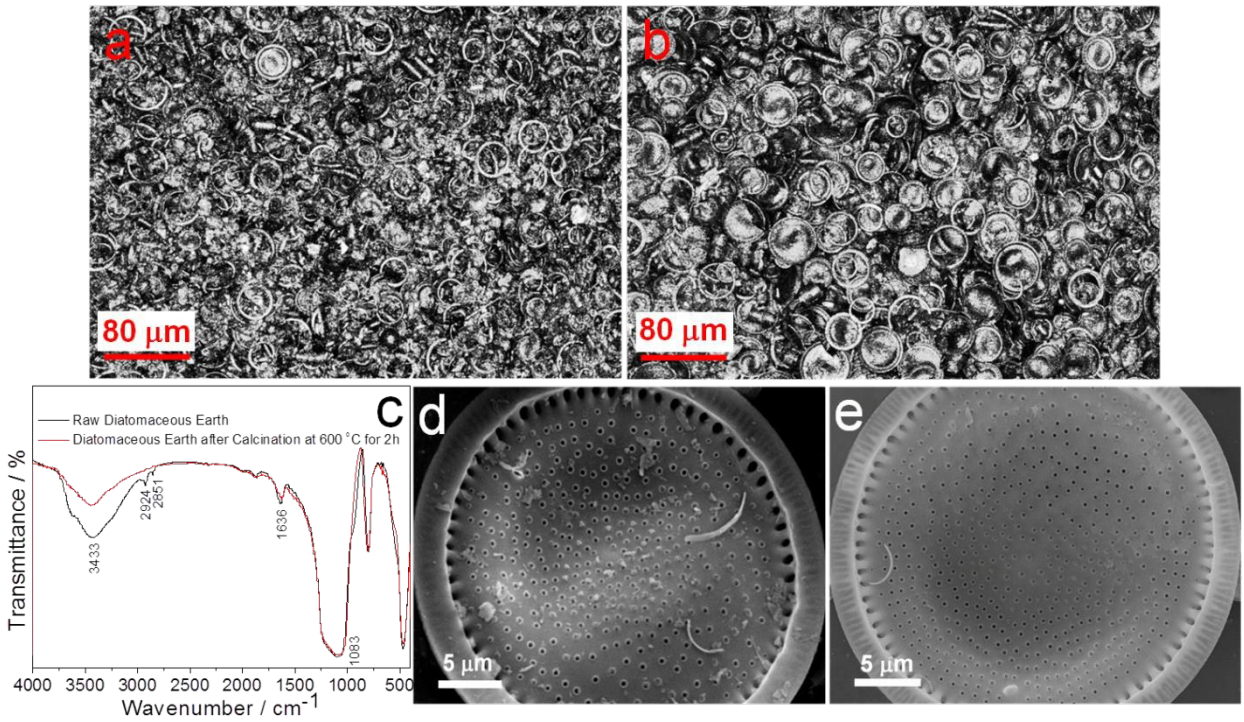

Figure 1 Confocal laser images of (a) raw diatomaceous earth and (b) raw diatomaceous earth after separation by low speed centrifugation in a saturated sucrose solution. (c) FT-IR spectra of diatomaceous earth before and after calcination at 600 ^{o}C for 2 h. (d) FE-SEM image of an intact fossil diatom frustule after the separation but before being calcined. (e) FE-SEM image of an intact fossil diatom frustule after the separation and calcination at 600 ^{o}C for 2 h.

3.2 Preparation of Au Nanoparticles of Two Different Sizes.

The TEM images, size distribution histograms, and UV-vis absorption spectra for the

two types of Au nanoparticles produced with different sizes are shown in Figure 2. According to Figure 2a, 2b, Au nanoparticles prepared by the method described in section 2.3.1 were nearly spherical and had a mean size of 18±2.4 nm with a relatively narrow size distribution (relative standard deviation (RSD) ~ 13%). Figure 2c, 2d show that monodisperse, almost spherical, Au nanoparticles with a larger mean diameter of 32±5.4 nm and a relatively uniform size distribution (RSD ~17%) were synthesized using the procedure in section 2.3.2. Figure 2e shows Au nanoparticle plasmon absorption band red shifts from 522 to 530 nm along with the increase of the nanoparticle size from 18±2.4 to 32±5.4 nm.

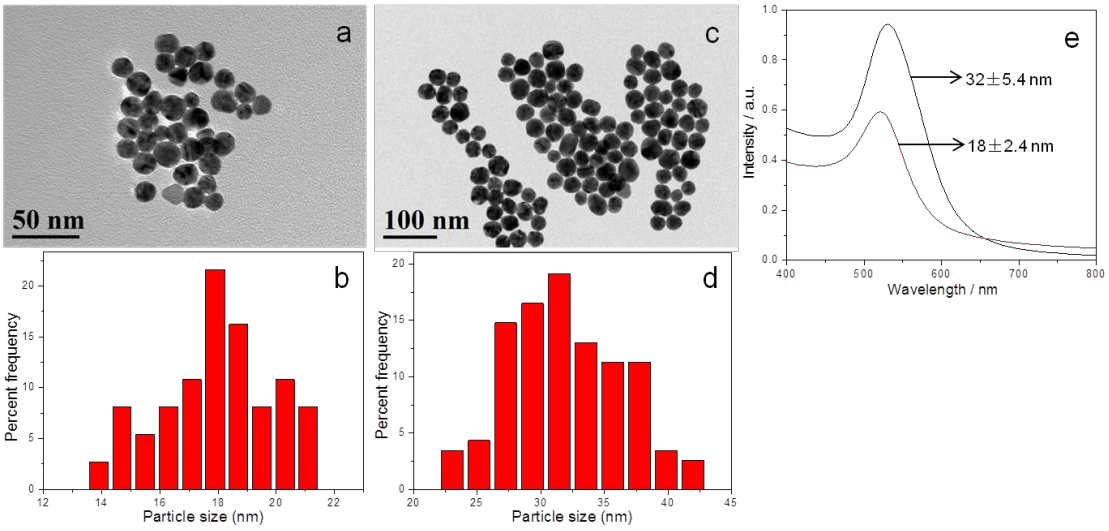

Figure 2 (a) TEM image and the corresponding (b) size distribution histogram of 18±2.4 nm Au nanoparticles. (c) TEM image and the corresponding (d) size distribution histogram of 32±5.4 nm Au nanoparticles. (e) UV-vis absorption spectra of 18±2.4 nm and 32±5.4 nm Au nanoparticles.

3.3 Assembly of Au Nanoparticles onto Amino-functionalized Diatomaceous Earth Templates and Fabrication of Portable Button-Like Tablets

The amino-silane functionalization of the fraction-free and ultra-high-purity diatomaceous earth templates and their interactions with the citrate-stabilized Au

nanoparticles, together with the formed portable button-like tablets used for the SERS detection of the chemical composition of the eccrine sweat in latent fingerprints were illustrated in Scheme 1. After the separation and purification, the fossil diatom frustules were modified by amino-silane, and their zeta potentials were investigated (Table 1). At first, raw diatomaceous earth and diatomaceous earth after separation and purification both have negative potentials due to the existence of silanol groups on the surface of the unfunctionalized diatomaceous earth. The zeta potential of the diatomaceous earth changed significantly to positive after the modification by APTES, indicating that amino-functionalized diatomaceous earth had been prepared. Then, the amino-functionalized diatomaceous earth templates were exposed to two sizes of citrate-stabilized Au nanoparticles that were negatively charged.

As we aim at SERS detection, the assembly of Au nanoparticles onto amino-functionalized diatomaceous earth templates should be uniformly separated and densely coated, which will ensure the reproducibility and high enhancement of the SERS signals. In Halas's work,[56] a systematical investigation of the influence of the solvent composition on the attachment of small gold nanoparticles to the amino-functionalized large silica nanoparticles was performed. Since the primary component of diatomaceous earth is silica, the solvent composition of 80% water and 20% ethanol was employed directly in our work by referring to Halas's work, as at this solvent composition, the attached gold nanoparticles were well-separated from their neighbors because of the appropriate ionic strength.[56] As for the "densely coated", different amounts of amino-functionalized diatomaceous earth were studied,

and the amount of 0.025 g was chosen (see Supporting Information for details).

The corresponding TEM images of diatomaceous earth-templated 18±2.4 and 32±5.4 nm Au nanoparticle arrays assembled under the optimal parameters are displayed in Figure 3a, 3b, showing that the two types of Au nanoparticles were uniformly and densely attached to the amino-functionalized diatomaceous earth templates following their surface morphologies *via* electrostatic interactions, and thus 3D periodically ordered diatomaceous earth-templated Au nanoparticle arrays have been successfully fabricated. Figure 3c, 3d shows TEM images of the corresponding control experiments in which diatomaceous earth after separation and purification but without the amino-silane functionalization was mixed with 18±2.4 and 32±5.4 nm Au nanoparticles. Figure 3c, 3d reveal that, except for the very few Au nanoparticles in the red circles that were accidentally adsorbed, both types of Au nanoparticles could hardly attach to diatomaceous earth templates, indicating that electrostatic interactions played a pivotal role in the assembly of Au nanoparticles. Compared to the amino-functionalized diatomaceous earth, the zeta potentials of diatomaceous earth-templated 18±2.4 and 32±5.4 nm Au nanoparticle arrays both decreased correspondingly because the attached citrate-stabilized Au nanoparticles were negatively charged (Table 1). The interactions between the diatomaceous earth and Au nanoparticles can be monitored by the naked-eye or UV-vis absorption spectra. When Au nanoparticles cannot be adsorbed onto the diatomaceous earth templates, after stirring and centrifugation, the supernatant still presents dark red (Figure 3e, left inset), and its UV-vis absorption spectrum exhibits a strong band (Figure 3e, the red curve);

whereas the supernatant will become light pink after the Au nanoparticles and diatomaceous earth have interacted with each other (Figure 3e, right inset), and the UV-vis absorption spectrum exhibits a very weak band (Figure 3e, the dark curve).[36] The digital camera images of raw diatomaceous earth, diatomaceous earth after the separation and purification, amino-functionalized diatomaceous earth, and diatomaceous earth-templated Au nanoparticle arrays are displayed in Figure 3f, and the diatomaceous earth-templated Au nanoparticle arrays present deep purple because of the coating of the Au nanoparticles. Figure 3g is the digital camera image of a portable SERS tablet formed by pressing the Au nanoparticle coated diatomaceous earth granulated composite material. The formed hard tablet is button-shaped with a diameter of 13 mm and a variable thickness depending on the amount of the granulated composite material used for the pressing (a fixed thickness of 2 mm was used throughout this work); it is robust, easy to carry around, and applicable to on-site SERS detections.

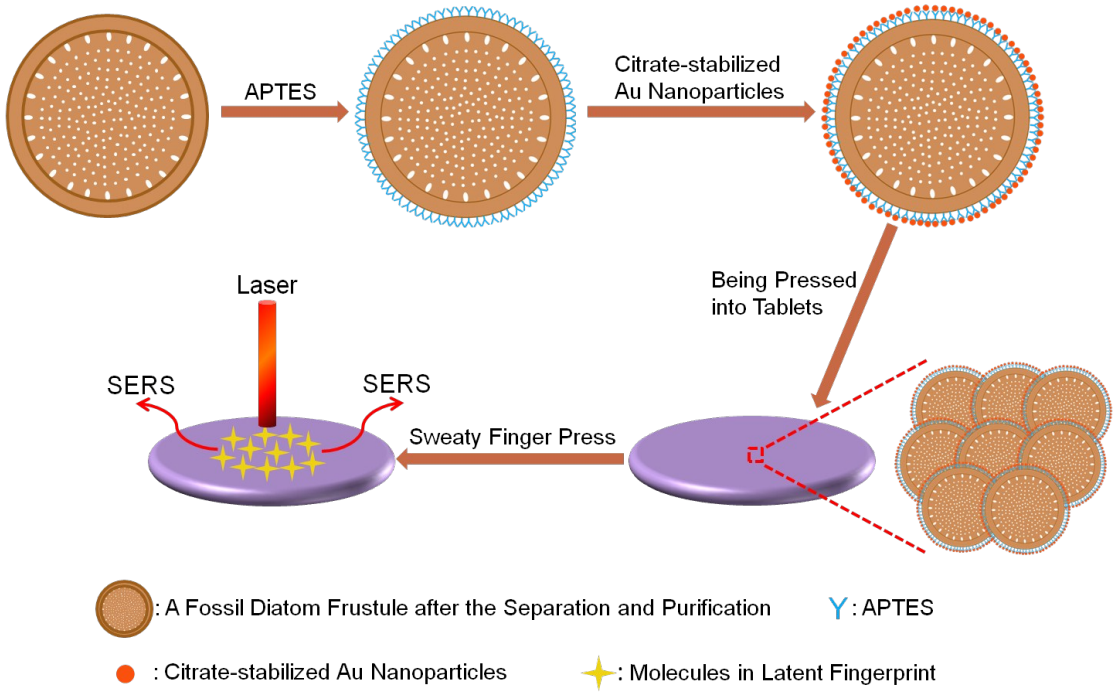

Scheme 1 Schematic diagram of the assembly of Au nanoparticles onto amino-functionalized diatomaceous earth templates and the fabricated button-like portable tablet for SERS detection of the chemical composition of eccrine sweat in latent fingerprints.

Table 1 Zeta Potential Values of Diatomaceous Earth and its Composite Materials[a]

Material	Zeta potential (mV)
Raw diatomaceous earth	-27.3 ±1.1
Diatomaceous earth after the separation and purification	-22.4 ±1.6
Amino-functionalized diatomaceous earth	42.7 ±3.5
Diatomaceous earth-templated 18 ±2.4 nm Au nanoparticle arrays	13.5 ±0.9
Diatomaceous earth-templated 32 ±5.4 nm Au nanoparticle arrays	6.24 ±0.5

[a] Values are averaged from three measurements

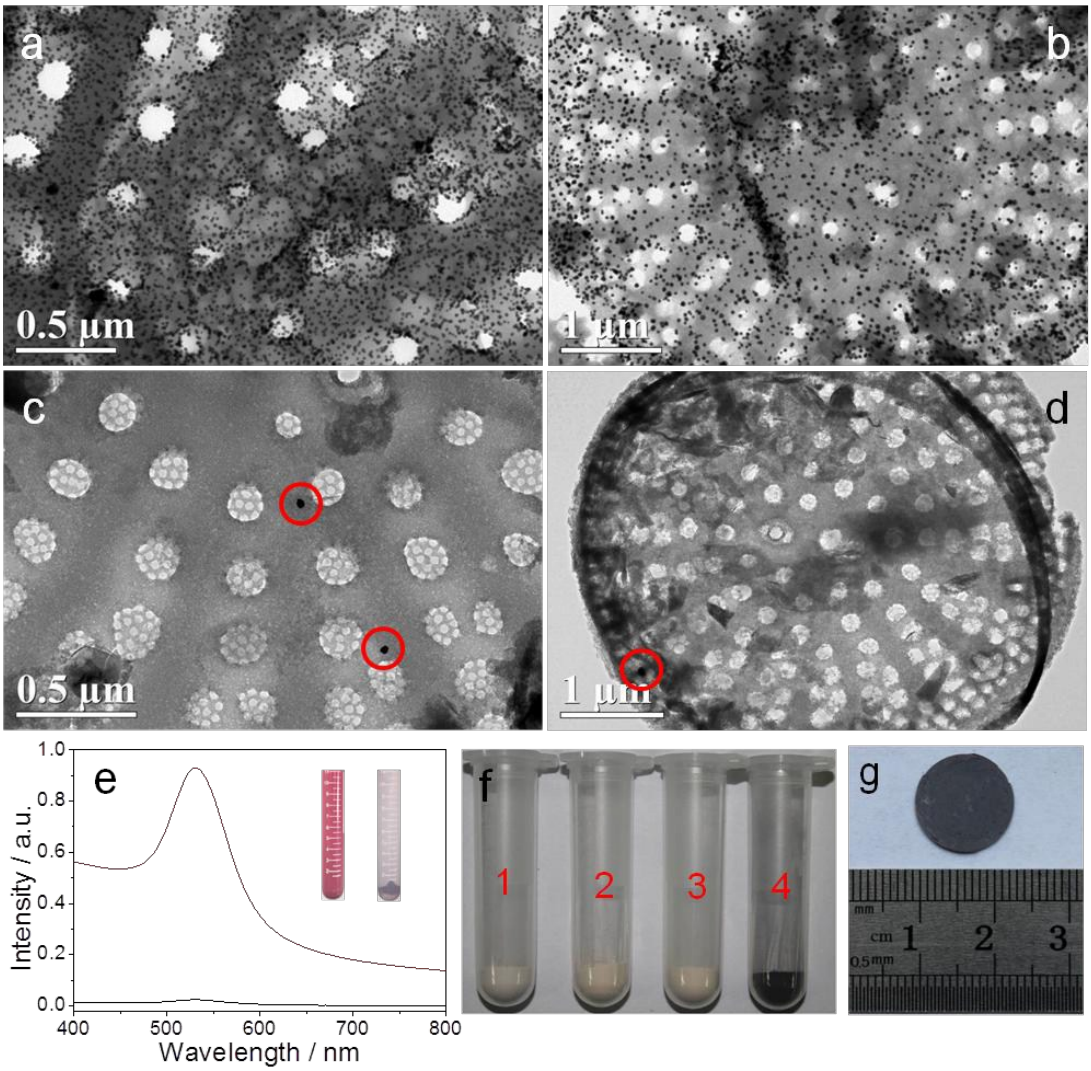

Figure 3 TEM images of amino-functionalized diatomaceous earth-templated (a) 18±2.4 and (b) 32±5.4 nm Au nanoparticle arrays. TEM images of the corresponding control experiments in which diatomaceous earth after separation and purification but without amino-silane functionalization were mixed with (c) 18±2.4 and (d) 32±5.4 nm Au nanoparticles; the very few Au nanoparticles in the red circles were accidentally adsorbed. (e) The supernatant of amino-functionalized diatomaceous earth-templated Au nanoparticle arrays in (a) and (b) appears light pink (right, inset) and exhibits a weak UV-vis absorption spectrum (the dark curve); the supernatant of the control experiments in (c) and (d) appears dark red (left, inset) and exhibits a strong UV-vis absorption spectrum (the red curve). (f) The digital camera images of (1) raw diatomaceous earth, (2) diatomaceous earth after separation and purification, (3) amino-functionalized diatomaceous earth, and (4) amino-functionalized diatomaceous earth-templated Au nanoparticle arrays. (g) The digital camera image of a button-like portable SERS tablet formed by pressing diatomaceous earth-templated Au nanoparticle array granulated composite material.

3.4 SERS Reproducibility

Reproducibility is an important index for the evaluation of SERS substrate performance. Here, R6G was selected as the probe molecule to test the reproducibility of the button-like portable SERS tablets composed of diatomaceous earth-templated 18±2.4 and 32±5.4 nm Au nanoparticle arrays. 10 μL of 10^{-4} M R6G solution was dropped onto the above two types of SERS tablets, and SERS spectra were acquired from 10 random spots on each SERS substrate under identical experimental conditions. From Figure 4a, 4b, the SERS spectra of R6G in these ten different positions are consistent with each other in terms of Raman peaks as well as Raman intensity. Figure 4c gives an even clearer clarification in that the RSDs of the peak intensity at 771 cm^{-1} are approximately 6.8% and 8.7% for Figure 4a and 4b, respectively. The low RSDs indicate good reproducibility and suggest that the button-like portable SERS substrates in this work are reliable and good candidates for the trace detection of the chemical composition of eccrine sweat in latent fingerprints.

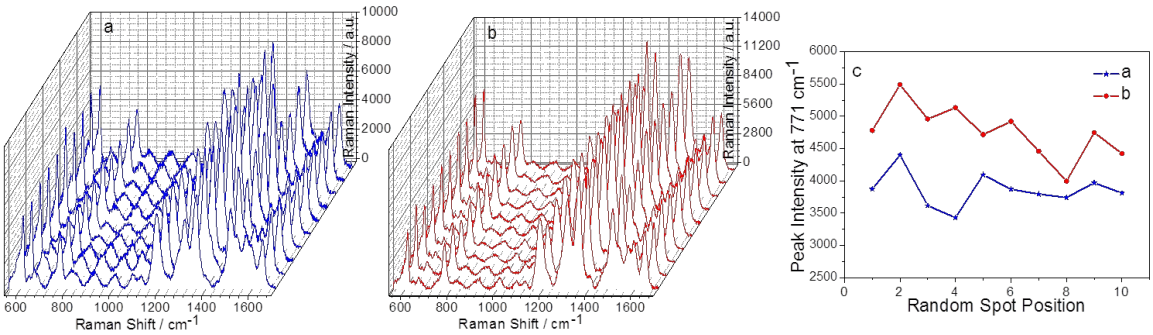

Figure 4 SERS spectra of 10^{-4} M R6G solution acquired from 10 random spots on the button-like portable SERS tablets composed of diatomaceous earth-templated (a) 18±2.4 and (b) 32±5.4 nm Au nanoparticle arrays. Excitation wavelength: 638 nm; laser power: 0.1 mW. (c) Plots of the peak intensities of R6G at 771 cm^{-1} obtained from 10 random spots on the abovementioned two portable SERS substrates.

3.5 EF Calculations, Relationship between SERS Intensity and R6G Concentration, and Enhancement Mechanism Analysis.

The EF is another key factor to assess the performance of SERS substrates. Here,

R6G was employed as the probe molecules to evaluate the enhancement capabilities. By referring to the procedures we used before,[58-61] the portable SERS tablets composed of diatomaceous earth-templated 18±2.4 and 32±5.4 nm Au nanoparticle arrays were calculated as 1.99×10^7 and 2.78×10^7, respectively (see Supporting Information for details). The results testified that within the size range of tens of nanometers, larger Au nanoparticles would give a higher SERS enhancement, which was in agreement with previous studies.[62,63]

Next, a series of SERS spectra of R6G at different concentrations were detected to demonstrate the sensitivity of the two portable SERS tablets. From Figure 5a, 5b, the SERS spectral intensity decreases as the concentration decreases, and both of the diatomaceous earth-templated 18±2.4 and 32±5.4 nm Au nanoparticle arrays can realize a detection of 10^{-10} M R6G solution with a low laser power (0.1 mW).

As a control, a mass-equivalent amount of Au nanoparticles was dripped directly onto the naked glass substrate. Because of the surface tension and "edge effects", this Au nanoparticle covered substrate tends to be non-uniform and forms aggregates (Figure S3a, S3b). Figure S3c, S3d show the SERS spectra of 10^{-4} M R6G solution acquired from 10 random spots on 18±2.4 and 32±5.4 nm Au nanoparticle covered glass substrates under identical experimental conditions, respectively. From Figure S3c, S3d, the SERS spectra of R6G in these ten different positions are consistent with each other in terms of Raman peaks, but vary considerably in Raman intensity, indicating a broad distribution in SERS EF values. Figure S3e gives an even clearer clarification, from which the RSDs of the peak intensity at 773 cm^{-1} are approximately 56.6% and

62.2% for Figure S3c and S3d, respectively. The high RSDs indicate the poor reproducibility of the Au nanoparticle covered glass substrates. Furthermore, the average EFs of the 18±2.4 and 32±5.4 nm Au nanoparticle covered substrates were calculated as 8.83×10^6 and 1.49×10^7, respectively. Next, as for the template-assisted SERS substrate fabrication, some other interestingly naturally occurring nanostructures were also employed. For example, in Stoddart's work, cicada wings were used as the template for the fabrication of the SERS substrate, with an EF of approximately 10^6.[64] Garrett *et al.* reported that the Graphium butterfly wing was used as a template for SERS substrate fabrication, and the EF was calculated to be 1.9×10^6 for gold.[65]

Hence, compared to the mass-equivalent amount of Au nanoparticles supported on a glass substrate, diatomaceous earth-templated 18±2.4 and 32±5.4 nm Au nanoparticle arrays in this work present higher EFs and much better reproducibilities, which is in agreement with Lee's result[66] and Schmit's report[67]. In Lee's work, gold-coated ZnO composite nanoarrays presented much higher SERS EFs than Au nanoparticle aggregates.[66] In Schmit's work, a larger SERS signal was observed on Au nanoparticle coated buoyant silica bubbles than on the aggregated colloidal Au nanoparticles.[67] Compared to some other natural templates, such as cicada wings and butterfly wings, diatomaceous earth template-assisted SERS substrates also show higher EFs. The reasons for the higher EFs upon using diatomaceous earth as a template can be explained from the following aspects. (1) Diatomaceous earth has a high specific surface area (19.9843 m^2/g after calcination at 600 ^oC for 2 h). Thus,

abundant Au nanoparticles can be fully adsorbed, not only on the surface but also around the pores of the diatomaceous earth (Figure S4). (2) When citrate-stabilized Au nanoparticles are very close to each other, the strong electrostatic repulsive force would make the neighboring capping ligands instantaneously stripped off, which generates some naked area on the surface of the Au nanoparticles. To decrease the surface free energy, these naked areas would weld to each other,[58, 68] thus resulting in the loss of the "hot spots".[69] The appropriate spacing between Au nanoparticles on diatomaceous earth template ensures that no welding happens between neighboring Au nanoparticles, and thus more "hot spots" can be created for SERS enhancement. Therefore, diatomaceous earth-templated Au nanoparticle arrays present higher EFs than the mass-equivalent amount of Au nanoparticles supported on glass substrates. (3) More adsorbed Au nanoparticles, together with the appropriate interparticle distances making sure that no interparticle welding occurs, enable a larger surface area of Au nanoparticles to expose on the diatomaceous earth template, thus resulting in more analyte molecules adsorbing.[70]

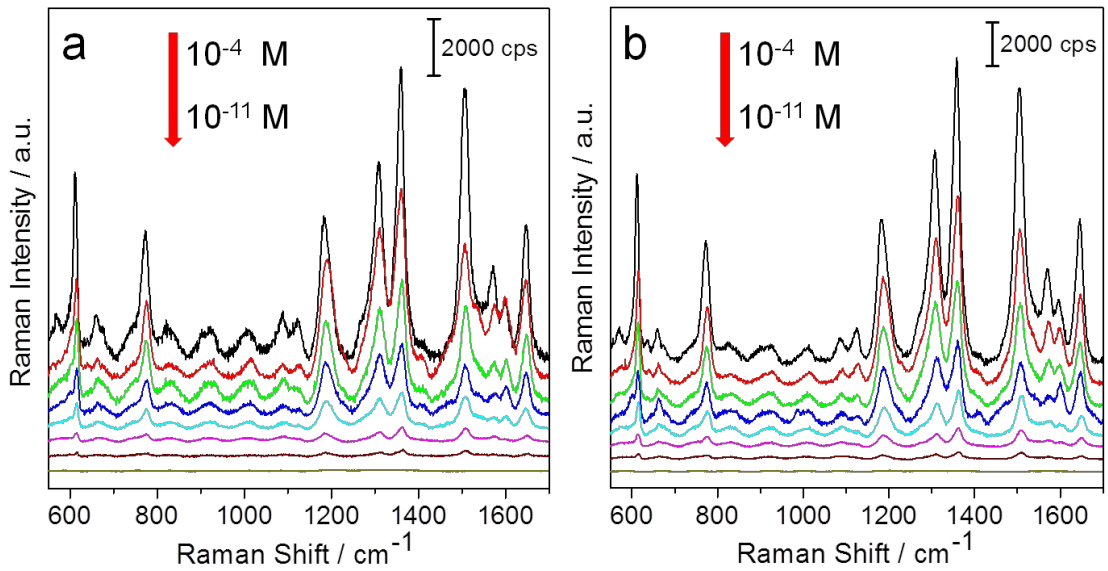

Figure 5 Concentration-dependent SERS spectra of R6G (10^{-11}~10^{-4} M), which were obtained from the portable SERS tablets composed of diatomaceous earth-templated (a) 18±2.4 and (b) 32±5.4 nm Au nanoparticle arrays. Excitation wavelength: 638 nm; laser power: 0.1 mW.

3.6 Long-Term Stability

Long-term stability is also a significant index for SERS substrates, as an ideal SERS sensor system needs a long time stable running without the loss of enhancement or degradation. Here, the two types of button-like portable SERS tablets composed of diatomaceous earth-templated 18±2.4 and 32±5.4 nm Au nanoparticle arrays were detected after they were saved in sterile petri dishes in the dark at room temperature for 90 days, and R6G was used as the probe molecule. Each SERS spectrum in Figure 6 is an average result of ten detections within each SERS substrate. After 90 days, the enhancement of SERS substrates composed of diatomaceous earth-templated 18±2.4 (Figure 6a) and 32±5.4 nm (Figure 6b) Au nanoparticle arrays were reduced by 43.6% and 42.5%, respectively (average results of the vibration mode at 771 cm^{-1}, 1187 cm^{-1}, and 1506 cm^{-1}), compared to the SERS spectra obtained from the freshly prepared substrates (Figure S2b, S2c). The long-term stability data of diatomaceous earth-templated 18±2.4 and 32±5.4 nm Au nanoparticle arrays are comparable to those of Halas's work[71] and Kim's work[72], in which the SERS enhancements were reduced by 50% and 40% after 90 days, respectively. The loss in SERS enhancement may be ascribed to the oxidization of Au nanoparticles in the air, and the decrease of the number of "hot spots" resulting from the surface diffusion of Au atoms and the interparticle welding process.[68]

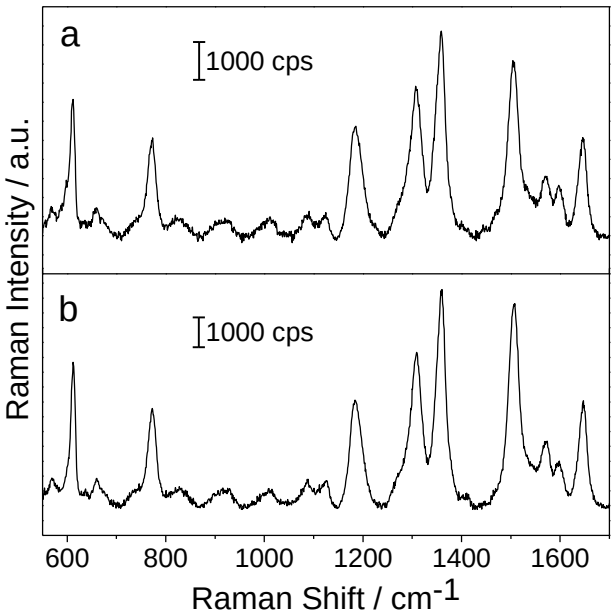

Figure 6 SERS spectrum of 10^{-4} M R6G solution acquired from button-like portable SERS tablets composed of diatomaceous earth-templated (a) 18±2.4 and (b) 32±5.4 nm Au nanoparticle arrays after they were saved in sterile petri dishes in the dark at room temperature for 90 days. Laser power: 0.1 mW.

3.7 SERS Analysis of the Chemical Composition of Eccrine Sweat in Latent Fingerprints.

The portable SERS tablet composed of diatomaceous earth-templated 32±5.4 nm Au nanoparticle arrays, which has a higher EF, was applied to analyze the chemical composition of eccrine sweat in latent fingerprints. A clean sweaty finger was pressed onto the portable SERS tablet, and SERS spectra were acquired immediately from the latent fingerprint. Figure 7a is the corresponding recorded SERS spectrum after the subtraction of substrate interference, which was well obtained with a good ratio of signal to noise under low incident laser power (1 mW) at 638 nm. As a control, Figure 7b (after the subtraction of substrate interference) is also the SERS spectrum of eccrine sweat in latent fingerprints but acquired from a glass substrate covered with a mass-equivalent amount of 32±5.4 nm Au nanoparticles. It was facile for us to obtain the SERS spectra of latent fingerprints from diatomaceous earth-templated Au

nanoparticle arrays rather than from the Au nanoparticle covered glass substrate, which may result from the higher EF and uniformity of the former SERS substrate. Comparing Figure 7a with Figure 7b, they basically match well with each other, even though they were obtained from different SERS substrates, indicating the reliability of the SERS technique. The SERS spectra with sharp and distinguishable vibrational bands in Figure 7a, 7b delivered the inherent chemical information, especially the molecular vibrational structures. The detailed assignments of the SERS bands in Figure 7a, 7b were interpreted in Table 2, giving us an idea of what chemical groups are in the eccrine sweat of latent fingerprints. Furthermore, by comparing the fingerprint SERS spectrum with the Raman spectrum of the analyte of interest, we can obtain a preliminary result on whether this analyte is contained in the eccrine sweat of latent fingerprints, assisting in medical diagnostics. The flat spectrum feature in Figure 7c is the Raman spectrum of eccrine sweat in latent fingerprints acquired on a glass substrate, indicating without the existence of the intense electromagnetic enhancement arising from surface plasmon resonances between Au nanoparticles that the Raman signals of the chemical composition of eccrine sweat in latent fingerprints cannot be enhanced and thus cannot be obtained.

As a tentative exploration, the successful analysis of microgram levels of the components of eccrine sweat in a latent fingerprint using the SERS substrate developed in this work suggests that the SERS-based methodology can have wide applications in the analysis of the trace components in latent fingerprints and can be potentially developed into a complementary technique for many researches. Future

work of SERS analysis in latent fingerprints can be performed in the following two main aspects: the structural analysis and the chemical analysis. The structural analysis: (1) determining what chemical groups are in a latent fingerprint; (2) the identification of the secondary structure of the proteins and polypeptides in latent fingerprints can be carried out by combining fingerprint SERS spectra with related techniques in molecular biology, because the Raman bands are closely related to the structures of the proteins and polypeptides.[77] The chemical analysis: (1) the latent fingerprint SERS analysis can be used for forensic investigations, such as drugs of abuse and explosive residues, by matching spectra to the known databases; (2) if the SERS-based methodology is combined with mass spectrometry, the specific proteins and polypeptide in latent fingerprints can be targeted, which can reveals the physical condition of an individual and can be further used in the medical diagnostics.

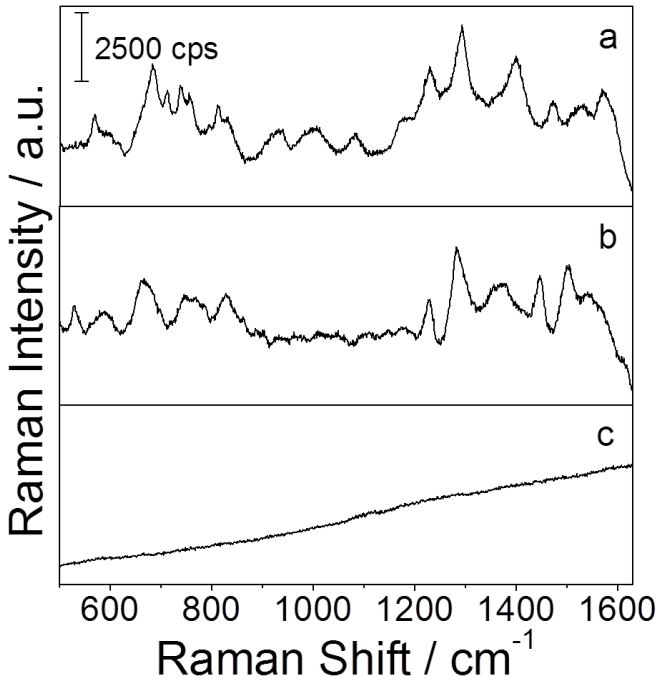

Figure 7 SERS spectrum of eccrine sweat in a latent fingerprint after the subtraction of the substrate interference, which was acquired from (a) the button-like portable SERS substrate composed of diatomaceous earth-templated 32±5.4 nm Au

nanoparticle arrays, and (b) a glass substrate covered with a mass-equivalent amount of 32±5.4 nm Au nanoparticles. Excitation wavelength: 638 nm; laser power: 1 mW. (c) Raman spectrum of eccrine sweat in a latent fingerprint acquired from a glass substrate. Excitation wavelength: 638 nm; laser power: 10 mW.

Table 2 Tentative Band Assignments for the SERS Spectra of Eccrine Sweat in Latent Fingerprints [73-76]

diatomaceous earth-templated 32±5.4 nm Au nanoparticle arrays	32±5.4 nm Au nanoparticle covered glass substrate	Assignments
Raman Shift / cm^{-1}		
	528	S-S stretch
566	581	Glycosidic ring
685	669	N-H bend
737	745	C-C stretch
814	823	C-H out-of-plane bend
1232	1229	C-N stretch
1293	1286	C-H deformation
1397	1378	α-amino acids
	1449	$-CH_2$, $-CH_3$ bend
1478		Aromatic rings stretch
1522	1506	N-H deformation
1568		N-H bend in primary amines and amides

4. Conclusions

Fraction-free and ultra-high-purity diatomaceous earth was successfully prepared by low speed centrifugation in saturated sucrose solution and calcination at 600 ^{o}C for 2 h. The prepared citrate-stabilized 18±2.4 and 32±5.4 nm Au nanoparticles were singly-attached and densely and uniformly distributed on the amino-functionalized diatomaceous earth templates. The formed 18±2.4 and 32±5.4 nm Au nanoparticle coated diatomaceous earth granulated composite materials were pressed into hard, button-like tablets with a fixed diameter of 13 mm and a thickness of 2 mm. Then, their SERS reproducibility, EFs, and long-term stability were evaluated. Finally, the button-like portable tablet composed of diatomaceous earth-templated 32±5.4 nm Au

nanoparticle arrays was successfully used for the SERS analysis of the chemical composition of eccrine sweat in a latent fingerprint, suggesting that the SERS-based methodology can have wide applications in the analysis of the trace components in latent fingerprints, assisting in medical diagnostics and forensic investigations.

***Supporting Information Available*:** Exploration of the appropriate amount of amino-functionalized diatomaceous earth templates used for the assembly of Au nanoparticles. EFs calculation of the two button-like portable SERS tablets composed of diatomaceous earth-templated 18±2.4 and 32±5.4 nm Au nanoparticle arrays. FE-SEM images of the mass-equivalent amount of 18±2.4 and 32±5.4 nm Au nanoparticle covered glass substrates and their reproducibilities. TEM images of diatomaceous earth-templated 18±2.4 and 32±5.4 nm Au nanoparticle arrays, showing Au nanoparticles not only adsorb on the surface but also around the pores of the diatomaceous earth.

Acknowledgements

We thank Dr. Linru Xu from China Pharmaceutical University for the helpful discussion. This work was supported by the National Natural Science Foundation of China (No. 50871028), Changjiang Scholars and Innovative Research Team in University (No. IRT0713), and the Fundamental Research Funds for the Central Universities (No. N110610001 and N141008001). J. Chen appreciates Northeastern University excellent doctoral dissertation breeding program, China.

References

[1] Xu, L. R.; Li, Y.; Wu, S. Z.; Liu, X. H.; Su, B. *Angew. Chem. Int. Ed.* 2012, 51,

8068-8072.

[2] Song, W.; Mao, Z.; Liu, X. J.; Lu, Y.; Li, Z. S.; Zhao, B.; Lu, L. H. *Nanoscale* 2012, 4, 2333-2338.

[3] Antoine, K. M.; Mortazavi, S.; Miller, A. D.; Miller, L. M. *J. Forensic Sci.* 2010, 55, 513-518.

[4] Burow, D.; Seifert, D.; Cantu, A. A. *J. Forensic Sci.* 2003, 48, 1094-1100.

[5] Lewis, L. A.; Smithwick, R. W.; Devault, G. L.; Bolinger, B.; Lewis, S. A. *J. Forensic Sci.* 2001, 46, 241-246.

[6] Bouldin, K. K.; Menzel, E. R.; Takatsu, M.; Murdock, R. H. *J. Forensic Sci.* 2000, 45, 1239-1242.

[7] Gao, D. M.; Li, F.; Song, J. X.; Xu, X. Y.; Zhang, Q. X.; Niu, L. *Talanta* 2009, 80, 479-483.

[8] Jaber, N.; Lesniewski, A.; Gabizon, H.; Shenawi, S.; Mandler, D.; Almog, J. *Angew. Chem. Int. Ed.* 2012, 51, 12224-12227.

[9] Qin, G.; Zhang, M. Q.; Zhang, T.; Zhang, Y.; Mclntosh, M.; Li, X.; Zhang, X. J. *Electroanal.* 2012, 24, 1027-1032.

[10] Shan, X. N.; Patel, U.; Wang, S. P.; Iglesias, R.; Tao, N. J. *Science* 2010, 327, 1363-1366.

[11] Bhargava, R.; Perlman, R. S.; Fernandez, D. C.; Levin, I. W.; Bartick, E. G. *Anal. Bioanal. Chem.* 2009, 394, 2069-2075.

[12] Day, J. S.; Edwards, H. G. M.; Dobrowski, S. A.; Voice, A. M. *Spectrochim. Acta. A* 2004, 60, 563-568.

[13] Chen, T. C.; Schultz, Z. D.; Levin, I. W. *Analyst* 2009, 134, 1902-1904.

[14] West, M. J.; Went, M. J. *Spectrochim. Acta. A* 2009, 71, 1984-1988.

[15] Croxton, R. S.; Baron, M. G.; Butler, D.; Kent, T.; Sears, V. G. *J. Forensic Sci.* 2006, 51, 1329-1333.

[16] Akiba, N.; Saitoh, N.; Kuroki, K.; Akiba, N.; Saitoh, N.; Kuroki, K. *J. Forensic Sci.* 2007, 52, 1103-1106.

[17] Ricci, C.; Phiriyavityopas, P.; Curum, N.; Chan, K. L. A.; Jickells, S.; Kazarian, S. G. *Appl. Spectrosc.* 2007, 61, 514-522.

[18] Croxton, R. S.; Baron, M. G.; Butler, D.; Kent, T.; Sears, V. G. *Forensic Sci. Int.* 2010, 199, 93-102.

[19] Kleinman, S. L.; Ringe, E.; Valley, N.; Wustholz, K. L.; Phillips, E.; Scheidt, K. A.; Schatz, G. C.; Van Duyne, R. P. *J. Am. Chem. Soc.* 2011, 133, 4115-4122.

[20] Lim, D. K.; Jeon, K. S.; Kim, H. M.; Nam, J. M.; Suh, Y. D. *Nat. Mater.* 2010, 9, 60-67.

[21] Sanles-Sobrido, M.; Exner, W.; Rodriguez-Lorenzo, L.; Rodriguez-Gonzalez, B.; Correa-Duarte, M. A.; Alvarez-Puebla, R. A.; Liz-Marzan, L. M. *J. Am. Chem. Soc.* 2009, 131, 2699-2705.

[22] Lu, L.; Eychmuller, A. *Accounts Chem. Res.* 2008, 41, 244-253.

[23] Zhang, R.; Zhang, Y.; Dong, Z. C.; Jiang, S.; Zhang, C.; Chen, L. G.; Zhang, L.; Liao, Y.; Aizpurua, J.; Luo, Y.; Yang, J. L.; Hou, J. G. *Nature* 2013, 498, 82-86.

[24] Wang, Y. Q.; Yan, B.; Chen, L. X. *Chem. Rev.* 2013, 113, 1391-1428.

[25] Liu, H. L.; Yang, Z. L.; Meng, L. Y.; Sun, Y. D.; Wang, J.; Yang, L. B.; Liu, J. H.;

Tian, Z. Q. *J. Am. Chem. Soc.* 2014, 136, 5332-5341.

[26] Zhang, X. Y.; Zhao, J.; Whitney, A. V.; Elam, J. W.; Van Duyne, R. P. *J. Am. Chem. Soc.* 2006, 128, 10304-10309.

[27] Duan, H. G.; Hu, H. L.; Kumar, K.; Shen, Z. X.; Yang, J. K. W. *ACS Nano* 2011, 5, 7593-7600.

[28] Hatab, N. A.; Hsueh, C. H.; Gaddis, A. L.; Retterer, S. T.; Li, J. H.; Eres, G.; Zhang, Z. Y.; Gu, B. H. *Nano Lett.* 2010, 10, 4952-4955.

[29] Hu, M.; Ou, F. S.; Wu, W.; Naumov, I.; Li, X. M.; Bratkovsky, A. M.; Williams, R. S.; Li, Z. Y. *J. Am. Chem. Soc.* 2010, 132, 12820-12822.

[30] Caldwell, J. D.; Glembocki, O.; Bezares, F. J.; Bassim, N. D.; Rendell, R. W.; Feygelson, M.; Ukaegbu, M.; Kasica, R.; Shirey, L.; Hosten, C. *ACS Nano* 2011, 5, 4046-4055.

[31] Pasquale, A. J.; Reinhard, B. M.; Dal Negro, L. *ACS Nano* 2011, 5, 6578-6585.

[32] Ou, F. S.; Hu, M.; Naumov, I.; Kim, A.; Wu, W.; Bratkovsky, A. M.; Li, X. M.; Williams, R. S.; Li, Z. Y. *Nano Lett.* 2011, 11, 2538-2542.

[33] Qian, C.; Ni, C.; Yu, W. X.; Wu, W. G.; Mao, H. Y.; Wang, Y. F.; Xu, J. *Small* 2011, 7, 1801-1806.

[34] Liberman, V.; Yilmaz, C.; Bloomstein, T. M.; Somu, S.; Echegoyen, Y.; Busnaina, A.; Cann, S. G.; Krohn, K. E.; Marchant, M. F.; Rothschild, M. *Adv. Mater.* 2010, 22, 4298-4302.

[35] Kleinman, S. L.; Frontiera, R. R.; Henry, A. I.; Dieringer, J. A.; Van Duyne, R. P. *Phys. Chem. Chem. Phys.* 2013, 15, 21-36.

[36] Rosi, N. L.; Thaxton, C. S.; Mirkin, C. A. *Angew. Chem. Int. Ed.* 2004, 43, 5500-5503.

[37] Payne, E. K.; Rosi, N. L.; Xue, C.; Mirkin, C. A. *Angew. Chem. Int. Ed.* 2005, 44, 5064-5067.

[38] Berry, V.; Rangaswamy, S.; Saraf, R. F. *Nano Lett.* 2004, 4, 939-942.

[39] Mao, C. B.; Flynn, C. E.; Hayhurst, A.; Sweeney, R.; Qi, J. F.; Georgiou, G.; Iverson, B.; Belcher, A. M. *Proc. Natl. Acad. Sci. U.S.A.* 2003, 100, 6946-6951.

[40] Bigall, N. C.; Reitzig, M.; Naumann, W.; Simon, P.; Van Pee, K. H.; Eychmuller, A. *Angew. Chem. Int. Ed.* 2008, 47, 7876-7879.

[41] Lang, Y.; Finn, D. P.; Caruso, F.; Pandit, A. *RSC Adv.* 2014, 4, 44418-44422.

[42] Chandrasekaran, S.; Sweetman, M. J.; Kant, K.; Skinner, W.; Losic, D.; Nann, T.; Voelcker, N. H. *Chem. Commun.* 2014, 50, 10441-10444.

[43] Nassif, N.; Livage, J. *Chem. Soc. Rev.* 2011, 40, 849-859.

[44] Gordon, R.; Losic, D.; Tiffany, M. A.; Nagy, S. S.; Sterrenburg, F. A. S. *Trends Biotechnol.* 2009, 27, 116-127.

[45] Jantschke, A.; Herrmann, A. K.; Lesnyak, V.; Eychmuller, A.; Brunner, E. *Chem. Asian J.* 2012, 7, 85-90.

[46] De Stefano, L.; Rendina, I.; De Stefano, M.; Bismuto, A.; Maddalena, P. *Appl. Phys. Lett.* 2005, 87, 233902.

[47] Losic, D.; Mitchell, J. G.; Voelcker, N. H. *Adv. Mater.* 2009, 21, 2947-2958.

[48] Yu, Y.; Addai-Mensah, J.; Losic, D. *J. Nanosci. Nanotechno.* 2011, 11, 10349-10356.

[49] Schlucker, S. *Surface Enhanced Raman Spectroscopy: Analytical, Biophysical and Life Science Applications*; Wiley-VCH Verlag GmbH & Co. KGaA, Weinheim, Germany, 2011.

[50] Jang, S.; Park, J. S.; Shin, S.; Yoon, C.; Choi, B. K.; Gong, M. S.; Joo, S. W. *Langmuir* 2004, 20, 1922-1927.

[51] Krug, J. T.; Wang, G. D.; Emory, S. R.; Nie, S. M. *J. Am. Chem. Soc.* 1999, 121, 9208-9214.

[52] Wang, J. A.; Zhu, T.; Zhang, X.; Liu, Z. F. *Acta Phys. Chim. Sin.* 1999, 15, 476-480.

[53] dos Santos, D. S.; Alvarez-Puebla, R. A.; Oliveira, O. N.; Aroca, R. F. *J. Mater. Chem.* 2005, 15, 3045-3049.

[54] Bastus, N. G.; Comenge, J.; Puntes, V. *Langmuir* 2011, 27, 11098-11105.

[55] Ji, X. H.; Song, X. N.; Li, J.; Bai, Y. B.; Yang, W. S.; Peng, X. G. *J. Am. Chem. Soc.* 2007, 129, 13939-13948.

[56] Westcott, S. L.; Oldenburg, S. J.; Lee, T. R.; Halas, N. J. *Langmuir* 1998, 14, 5396-5401.

[57] Chen, J.; Yang, T.; Li, S.; Ren, Y. P.; Wang, J. H.; Qin, G. W. *Metallic Functional Materials* (in Chinese) 2012, 19, 32-35.

[58] Chen, J.; Shen, B.; Qin, G. W.; Hu, X. W.; Qian, L. H.; Wang, Z. W.; Li, S.; Ren, Y. P.; Zuo, L. *J. Phys. Chem. C* 2012, 116, 3320-3328.

[59] Chen, J.; Qin, G. W.; Wang, J. S.; Yu, J. Y.; Shen, B.; Li, S.; Ren, Y. P.; Zuo, L.; Shen, W.; Das, B. *Biosens. Bioelectron.* 2013, 44, 191-197.

[60] Chen, J.; Shen, W.; Biswajit, D.; Li, Y. Y.; Qin, G. W. *RSC Adv.* 2014, 4, 22660-22668.

[61] Chen, J.; Qin, G. W.; Shen, W.; Li, Y. Y.; Biswajit, D. *J. Mater. Chem. C* 2015, 3, 1309-1318.

[62] Njoki, P. N.; Lim, I. I. S.; Mott, D.; Park, H. Y.; Khan, B.; Mishra, S.; Sujakumar, R.; Luo, J.; Zhong, C. J. *J. Phys. Chem. C* 2007, 111, 14664-14669.

[63] Jang, S. M.; Park, J. S.; Shin, S. M.; Yoon, C. J.; Choi, B. K.; Gong, M. S.; Joo, S. W. *Langmuir* 2004, 20, 1922-1927.

[64] Stoddart, P. R.; Cadusch, P. J.; Boyce, T. M.; Erasmus, R. M.; Comins, J. D. *Nanotechnology* 2006, 17, 680-686.

[65] Garrett, N. L.; Vukusic, P.; Ogrin, F.; Sirotkin, E.; Winlove, C. P.; Moger, J. *J. Biophoton.* 2009, 2, 157-166.

[66] Chen, L. M.; Luo, L. B.; Chen, Z. H.; Zhang, M. L.; Zapien, J. A.; Lee, C. S.; Lee, S. T. *J. Phys. Chem. C* 2010, 114, 93-100.

[67] Schmit, V. L.; Martoglio, R.; Scott, B.; Strickland, A. D.; Carron, K. T. *J. Am. Chem. Soc.* 2012, 134, 59-62.

[68] Qin, G. W.; Liu, J. C.; Balaji, T.; Xu, X. N.; Matsunaga, H.; Hakuta, Y.; Zuo, L.; Raveendran, P. J. *J. Phys. Chem. C* 2008, 112, 10352-10358.

[69] Andreussi, O.; Corni, S.; Mennucci, B.; Tomasi, J. *J. Chem. Phys.* 2004, 121, 10190-10202.

[70] Le Ru, E.; Etchegoin, P. *Principles of Surface Enhanced Raman Spectroscopy and Related Plasmonic Effects*; Elsevier, Amsterdam, 2009.

[71] Wang, H.; Levin, C. S.; Halas, N. J. *J. Am. Chem. Soc.* 2005, 127, 14992-14993.

[72] Choi, S.; Ahn, M.; Kim, J. *Anal. Chim. Acta* 2013, 779, 1-7.

[73] Pavia, D. L.; Lampman, G. M.; Kriz, G. S. *Introduction to Spectroscopy: A Guide for Students of Organic Chemistry, 2nd ed.*; Harcourt Brace College Publishers, Fort Worth, 1996.

[74] Braun, R. D. *Introduction to Instrumental Analysis*; Mcgraw-Hill College, 1987.

[75] Silverstein, R. M.; Webster, F. X. *Spectrometric Identification of Organic Compound, 6th ed.*; Wiley, New York, 1998.

[76] Solomons, T. W. G. Fryhle, C. *Organic Chemistry, 7th ed.*; Upgrade, Wiley, New York, 2001.

[77] Zhu, Z. Y.; Gu, R. A.; Lu, T. H. *The Application of Raman Spectroscopy in Chemistry (in Chinese)*; Northeastern University Press, Shenyang, China, 1998.

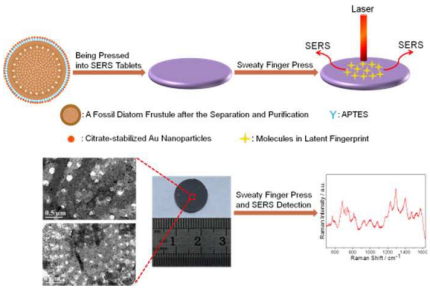

The button-like, periodically ordered SERS tablets were fabricated by pressing diatomaceous earth-templated Au nanoparticle arrays, and were used for the analysis of the trace chemical composition of eccrine sweat in latent fingerprints.